

Electronic structure and reflectance anisotropy spectrum of InAs(110)X. López-Lozano,¹ O. Pulci,² C. Noguez,^{3,*} K. Fleischer,⁴ R. Del Sole,² and W. Richter^{2,4}¹*Instituto de Física, Universidad Autónoma de Puebla, Apartado Postal J-48, Puebla 72570, México*²*INFN, Università di Roma Tor Vergata, Via della Ricerca Scientifica 1, I-00133 Roma, Italy*³*Instituto de Física, Universidad Nacional Autónoma de México, Apartado Postal 20-364, Distrito Federal 01000, México*⁴*TU-Berlin, Institut fuer Festkoerperphysik, Hardenbergstr. 36, D-10623 Berlin, Germany*

(Received 1 November 2004; published 31 March 2005)

The electronic structure of the InAs(110) surface is investigated using several theoretical tools: semiempirical tight-binding, density functional theory, and perturbative many-body theory within the GW approximation. Comparison is made with available photoemission data. Moreover, we calculate the optical properties of this surface and perform reflectance anisotropy experiments. The tight-binding and especially the GW approximations provide a very good description of the optical spectra and allow for a more detailed analysis of the origin of the spectral features.

DOI: 10.1103/PhysRevB.71.125337

PACS number(s): 78.68.+m, 73.20.-r, 68.47.Fg

I. INTRODUCTION

There is continuing interest in the electronic properties of III-V-surfaces because of the technological relevance of these materials. The (110) surface as a cleavage face is the most natural choice for basic studies of III-V compounds, since it is easily prepared in a well defined manner with a well defined stoichiometry, a feature nearly all other III-V surfaces do not have. On non-cleavage surfaces, experiments in general have to deal with the uncertainty of the exact surface status. The structure of all (110)-III-V-surfaces has already been studied both theoretically and experimentally for a long time and is very well known.¹⁻³ The surface relaxes in a (1 × 1) pattern with the surface cation atom moving inwards and the anion atom moving outwards. Larger bandgap III-V semiconductors of higher technological importance such as GaAs, GaN, InP, and GaP have been more widely studied.²⁻⁹ Less work has focused on the small bandgap materials InAs and InSb which, however, are also of technological interest (for infrared detection devices, for example).

Theoretically, InAs(110) has been studied mainly within the semiempirical tight-binding approach.¹⁰⁻¹³ Only a few papers deal with the *ab initio* theoretical investigation of the InAs(110) surface,¹⁴⁻¹⁶ and are limited to the use of density functional theory¹⁷ (DFT) within the local density approximation (LDA).¹⁸ The electronic structure and atomic positions of InAs(110) were calculated several years ago using a total-energy minimization scheme¹⁰ based on a semiempirical tight-binding (TB) approach. The reported electronic surface states, however, differ from available experimental measurements. One may argue that the discrepancies in the semiempirical calculations are due to the fact that they were performed using an atomic reconstruction that was not fully relaxed. Almost a decade later, an *ab initio* calculation¹⁴ was performed using the DFT-LDA approach, fully relaxing the geometry with a Car-Parrinello scheme.¹⁹ DFT is known to be a powerful tool in dealing with ground-state properties, but suffers from the well known gap problem in the determination of the electronic bands.^{20,21} Consequently, DFT calcu-

lation presents systematic underestimations of the electronic gaps when compared with experiment. In particular, a metallic behavior is predicted for bulk InAs, since a crossing of the conduction and valence bands appears at Γ within DFT, thus giving a negative gap.²²

The available experimental measurements^{1,23-32} focus mainly on the geometry and the electronic band structure of InAs(110). Andersson and collaborators^{24,25} measured the energies of occupied surface states at high-symmetry points using photoemission techniques. Independently, Swanson *et al.*²⁶ also performed a similar experiment, and found differences of up to 0.5 eV with those values reported by Andersson and collaborators.^{24,25} Few inverse photoemission investigations appear in the literature,²⁹⁻³¹ but are not angle resolved and suggest the existence of an empty surface state with energy ranging from 0.75 to 1.9 eV above the top of the valence band. The electronic gaps between surface states at the high symmetry points of the Brillouin zone have also been measured by Carstensen *et al.*²³ by performing direct and inverse photoemission spectroscopy on the same sample. However, the comparison between theory and the different photoemission measurements is in general still not satisfying.

The optical properties of InAs(110) have been also investigated by Shkrebtii and collaborators¹² several years ago within a combined semiempirical TB and experimental study, and recently by Vázquez-Nava *et al.*¹³ To our knowledge, those have been so far the only attempts to calculate the reflectance anisotropy spectrum (RAS) of InAs(110). The TB calculations and measured RAS spectra showed discrepancies, however, and call for further investigation.

In this work, we study in detail the electronic structure and optical properties of the InAs(110) surface, driven by the lack of *ab initio* calculations and the unsatisfactory agreement with experiment. Moreover, this system is simple enough to be used as a test case for several computational techniques, ranging from TB to DFT and a many-body approach, in order to assess the validity of the various schemes, with the perspective of studying more complex systems which are not accessible (yet) by many-body theory. We em-

ploy density functional theory for the ground state properties and many-body perturbation theory in the GW approximation^{20,21} for the excited state properties, namely optical properties and electronic structure. Comparison with new semiempirical TB results and new experimental optical data in an extended spectral range is performed.

II. EXPERIMENTAL DETAILS

InAs(110) samples ($8 \times 5 \times 5$ mm) were prepared from bulk InAs (n doping: 10^{-18} cm⁻³) by cleavage in ultrahigh vacuum (UHV) at a base pressure of 8×10^{-11} mbar. Reflectance anisotropy spectrum (RAS) measurements were performed through a low strain window in the UHV chamber by using the technique as proposed by Aspnes.³³ The RAS apparatus is equipped with MgF₂ Rochon polarizers, a CaF₂ photoelastic modulator, and two detector systems: a photomultiplier and accordingly a silicon/InGaAs double diode detector. As compared to standard set-ups the accessible spectral range is therefore enlarged from 0.8 up to 9 eV. However, absorption by the air in the open optical path and in the low strain optical view ports (quartz) of the UHV chamber, limits the range from 0.8 to 6.5 eV.

In order to compare not only the spectral shapes of calculations and measurements but also, quantitatively, the reflectance amplitudes, we calibrated our setup with the known optical anisotropy of quartz. We thereby utilized the front reflection from a quartz wedge at the later position of the InAs(110) sample. This procedure assured an accuracy of a few percent for the experimental data.

III. COMPUTATIONAL DETAILS

The equilibrium geometry has been found by fully relaxing the atomic position within a DFT-LDA Car-Parrinello scheme using a plane wave pseudopotential code³⁴ with an energy cutoff of 15 Ry. Test calculations using a GGA exchange and correlation potential did not show significant differences. The surface has been modeled by a slab consisting of 11 InAs layers plus seven layers of vacuum. The equilibrium geometry was used to perform electronic and optical calculations within semiempirical tight binding and many-body perturbation theory in the GW approximation.

For TB calculations the InAs(110) surface was modeled using several thicknesses up to a slab of 50 atoms. The electronic structure of the slab was calculated using a well-known parametrized TB approach with a sp^3s^* orbital-like basis, within a first-neighbor interaction.^{35,36} The TB approximation has been successfully applied for many years to calculate the electronic and optical properties of a variety of semiconductor surfaces, including other III-V compounds.⁸ The TB parameters are taken to be the same as those of Vogl³⁶ for the bulk but they are scaled by a factor of $(d_0/d)^2$, where d is the bond length of any two first-neighbor atoms, and $d_0 = \sqrt{3}a_0/4$ (Ref. 37). Our DFT theoretical lattice constant, a_0 , equal to 11.38 a.u., is to be compared with the experimental value of 11.41. These parameters provide a good description of the electronic structure of the valence bands and lowest conduction bands. Discrepancies only oc-

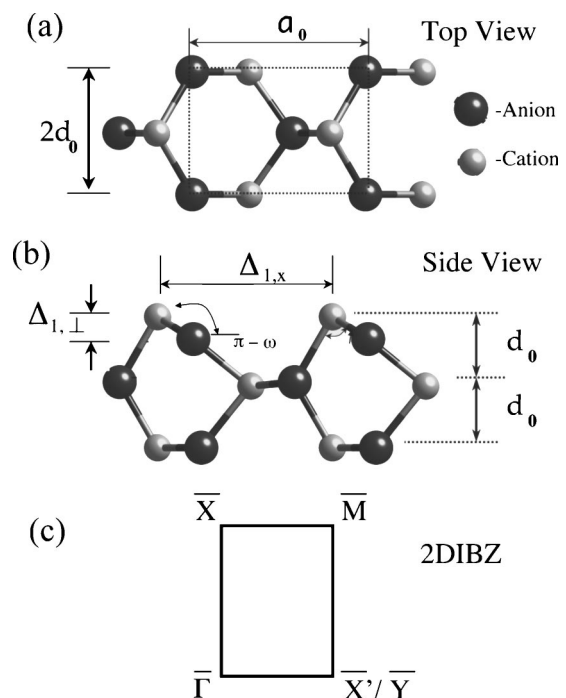


FIG. 1. Model of the atomic geometry of InAs(110). (a) Top view of a surface unit cell. (b) Side view of the first three atomic layers. (c) Two-dimensional irreducible Brillouin zone (2DIBZ). The calculated geometrical parameters are: $a_0 = 5.861$ Å, $\Delta_{1,\perp} = 0.75$ Å, $\Delta_{1,x} = 4.663$ Å, and $\omega = 32.0^\circ$.

cur for the higher conduction bands, and for the lowest two conduction bands along the X - W direction.³⁸

Within many-body perturbation theory, the quasiparticle (QP) energies have been calculated using the perturbative GW scheme,²¹ which involves computing the excited states energies as a first order perturbation correction to the DFT bands

$$\epsilon^{\text{QP}} = \epsilon^{\text{DFT}} + \langle \Sigma - V_{xc}^{\text{DFT}} \rangle \quad (1)$$

with $\Sigma = iGW$. We have used 800 empty bands, 13 k points in the irreducible part of the Brillouin zone (IBZ), and 1077 plane waves for the exchange and correlation part of the self-energy Σ . For the screening, a plasmon-pole model has been used.²¹ Optical properties have been calculated within the single quasiparticle scheme using 128 k points in the IBZ (corresponding to 128×4 in the full BZ). In the tight binding calculation we used up to 7000 k points in the IBZ.

IV. RESULTS

As in the other III-V semiconductors, the InAs(110) surface relaxes in such a way that the surface cation atom moves inwards to an approximately planar configuration, with its first-neighbor anion atoms in a threefold coordination [Figs. 1(a) and 1(b)]. The topmost anion atom moves outward to the surface, showing a pyramidal configuration with its three first-neighbors cation atoms.^{2,3} The calculated geometrical parameters that describe the relaxation of the surface atoms are in good agreement with experiment³² and with previous DFT-LDA calculations.¹⁴

TABLE I. Bulk electronic gaps at high symmetry points of the IBZ. Experimental values are taken from Ref. 39 except where noted.

	Γ	X	L	E'_0
DFT	-0.1	3.7	1.9	4.0
GW	0.4	4.3	2.5	4.6
TB	0.4	4.7	2.5	4.5
Exp. (Ref. 39)	~ 0.4	4.3 (Ref. 43)–4.7	2.5–2.6	4.4–4.6

A. Electronic band structure

As mentioned in the Introduction, DFT suffers from the well known problem of gap underestimation. This is even more critical in InAs, where DFT predicts metallic behavior for the bulk. Our calculations, in particular and in agreement with previous calculations,²² show also a negative bulk gap at Γ . For other gaps of InAs (Table I), DFT also gives values considerably lower than the experimental ones. Hence, InAs is a system where it is of crucial importance to overcome the shortcomings of DFT. TB values and GW corrections to the DFT bulk InAs gaps are also listed in Table I. The agreement of TB and GW with the range of gap values from experiments³⁹ is quite good, though experimental data are quite scattered at X . The agreement of the GW *ab initio* approach compared to DFT-LDA is especially noteworthy.

The surface electronic band structure is intimately related to the relaxation of the surface. Experimentally, the electronic structure can be determined by means of electron spectroscopies such as photoemission (PE), inverse photoemission (IPE), and scanning tunneling spectroscopy (STS). These techniques are sensitive to the surface features and electronic properties due to reconstructions or adsorption events. The GW results for the electronic gaps at the high symmetry points \bar{X} , \bar{M} , and \bar{X}' [see Fig. 1(c)] are shown in Table II and compared with the experimental data obtained by direct and inverse photoemission measurements on the same sample.²³ At $\bar{\Gamma}$ our calculations only found weak resonances, thus a comparison with the experimental results by Carstensen *et al.* (who found a 1.7 eV gap between surface states at Γ) was not possible. At the other high symmetry points (\bar{X} , \bar{M} , \bar{X}'), the agreement with experiment is excellent and within 0.2 eV. TB and DFT electronic gaps are also listed in Table II. The DFT values are on the average too low by 0.5 eV, while the TB gaps fit better at the \bar{M} and \bar{X}' points but show discrepancies with experiment at \bar{X} , possibly

TABLE II. Surface electronic gaps at high symmetry points of the 2D IBZ.

	\bar{X}	\bar{M}	\bar{X}'
DFT	1.8	2.1	2.0
GW	2.4	2.6	2.6
TB	3.1	2.6	2.3
Exp. (Ref. 23)	2.5	2.6	2.4

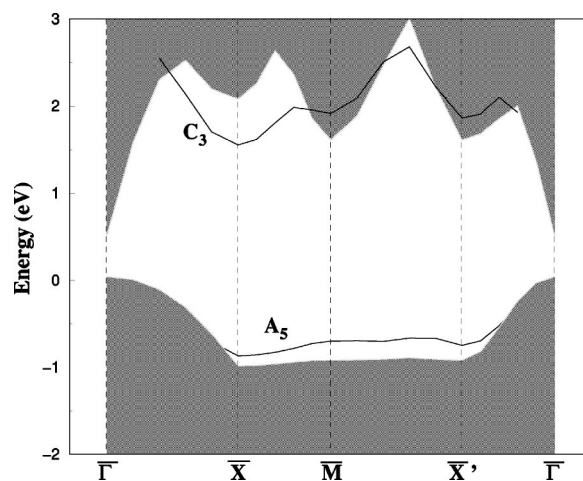


FIG. 2. GW electronic band structure of the reconstructed InAs(110) surface. Shaded regions represent the projected bulk states, while continuous lines represent surface electronic states.

because d orbitals are not included in the sp^3s^* TB calculation.³⁸

The GW electronic band structure along high-symmetry points of the 2D-IBZ of InAs(110) is shown in Fig. 2. The projected bulk electronic states are shown as gray shaded regions, while the surface electronic states are shown as black lines. We denote the surface electronic states using the labels A_5 and C_3 associated to the surface anions and cations, respectively, as introduced by Chelikowsky and Cohen.⁴⁰ The A_5 surface states correspond to the dangling bonds of the As atoms located at the first atomic layer. The A_5 states form a band from the high-symmetry point \bar{X} to the point \bar{X}' , going through the high-symmetry point \bar{M} in the 2D IBZ. This band has a minimum at \bar{X} with an energy of -0.9 eV (see Table III) and disperses upwards towards the $\bar{\Gamma}$ point. From \bar{X} , the band also disperses upwards towards the \bar{M} point, where the A_5 surface states have an energy of about -0.7 eV. The A_5 band shows a small dispersion between \bar{X} and \bar{X}' , giving rise to a large contribution to the density of states. Experimentally,²⁵ the A_5 surface state has a dispersion of about 0.15 eV from \bar{X} to \bar{X}' (through \bar{M}) which compares well with the calculated (GW) value of about 0.2 eV. The experimental energies of the A_5 band are also listed in Table III.

Above the valence band maximum (VBM) we found the unoccupied surface state band C_3 localized at the cations in the first few layers. It shows a strong p character due to the cation dangling bonds. At \bar{X} C_3 has a minimum with an energy of about 1.5 eV, and has a maximum value between \bar{M} and \bar{X}' at an energy of about 2.7 eV. Because of the large dispersion of C_3 , the joint density of surface states is not large. We find that these states do not contribute to the surface peaks in the calculated optical properties (see Sec. IV B).

Differences are seen in the dispersion when compared to TB. While our and previous¹⁴ DFT calculation, as well as our GW calculation, finds that C_3 has a minimum at \bar{X} , TB gives

TABLE III. Experimental and theoretical values of the surface states at high-symmetry points of the 2D IBZ. The energy values are in eV and the zero energy corresponds to the top of the valence band. The first two columns show our GW and TB results.

State	GW	TB	PE (Ref. 24)	PE (Ref. 25)	PE (Ref. 26)	DFT (Ref. 14)	TB (Ref. 10)
$A_5(\bar{\Gamma})$	-0.3		-0.30	-0.45	-0.53		-0.3
$A_5(\bar{X})$	-0.9	-1.21	-1.00	-1.15	-0.83	-0.85	-0.9
$A_5(\bar{X}')$	-0.7	-0.70	-0.85	-1.00	-0.73		-0.7
$A_5(\bar{M})$	-0.7	-0.81		-1.10	-0.70		-0.8
State	GW		TB			Exp.	
$\bar{\Gamma}$	2.0		2.0			1.9 (Ref. 29)	
$C_3(\bar{X})$	1.5		1.9				
$C_3(\bar{X}')$	1.9		1.3				
$C_3(\bar{M})$	1.9		1.3				
Surf state						0.75 (Ref. 30), 1.2 (Ref. 31)	

a maximum at the same symmetry point in agreement with other semiempirical calculations.^{10–12} GW calculations give an upward dispersion around \bar{X} , while in TB we find a downward dispersion. However, notice that the discrepancy between TB and other results is only at \bar{X} , possibly because d orbitals are not included in the present calculation.³⁸

Comparison with available experimental measurements is not straightforward. The electronic properties of InAs(110) have been investigated previously using inverse photoemission^{23,29–31} (IPE) spectroscopy. The few experiments on empty surface states, when not performed with angular resolution, are difficult to interpret. Measurements assigned an energy of 1.9 eV (Ref. 29) to a state at $\bar{\Gamma}$; empty surface states at 0.75 eV (Ref. 30) and 1.2 eV (Ref. 31) have also been measured, but without assignment to a specific k point of the BZ. Our GW and TB calculations find a surface resonance at $\bar{\Gamma}$ at 2.0 eV (in TB it has C_3 character). This is in good agreement with the observed 1.9 eV surface state of Ref. 29. On the other hand, neither GW nor TB finds surface states around 1.2 eV at any k point of the BZ.

In order to conclude more about the energy position and the dispersion of the empty states, further angle resolved inverse photoemission experiments are necessary. Concerning the different dispersion at \bar{X} found within GW and TB calculations, comparison with InP(110) and GaAs(110), where angle resolved photoemission experiments and GW calculations do exist, suggests that C_3 has indeed a minimum and not a maximum at the \bar{X} point.

B. Optical properties

The difference of the reflectance for light polarized in two different directions gives, for cubic crystals, a measure of dielectric anisotropy of the surface which has been shown to be very sensitive to the surface band structure and thus can serve as a test for the different calculations. The reflectance anisotropy is defined here as

$$\frac{\Delta R}{R_0} = \frac{R_{[\bar{1}10]} - R_{[001]}}{R_0} \quad (2)$$

with R_0 being the average isotropic reflectance.⁴¹ The details of the calculation are fully explained in Ref. 42.

The reflectance anisotropy spectrum (RAS) has contributions from electronic transitions between occupied and empty states involving both surface and modified bulk states. In Fig. 3(b) we compare the measured RAS spectrum of InAs(110) with the TB (a) and GW (c) calculation. As it is expected, TB shows good correlation with the experimental data but fails to describe the high energy end of RAS (above 5 eV), which might be related to the lack of d orbitals in the basis set, as discussed before. On the other hand, GW shows a remarkable agreement for all energies.

RAS shows a rich spectral structure since contributions from all kinds of electron transitions involving surface states as well as electron transitions involving modified bulk states

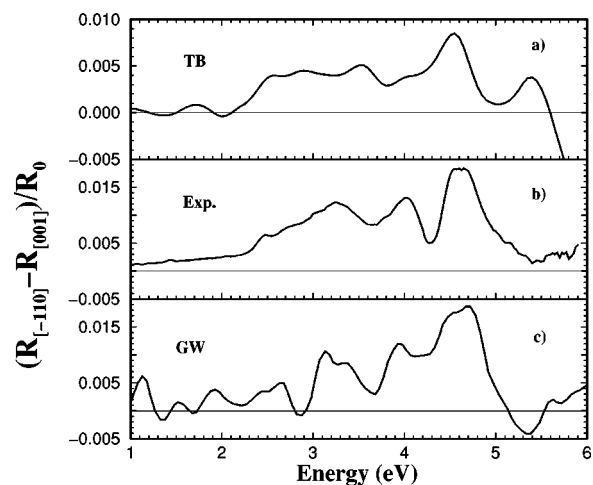


FIG. 3. Reflectance anisotropy spectra of InAs(110): (a) TB calculation, (b) experiment, (c) GW calculation. A broadening of 0.05 (0.2) eV has been used in the GW (TB) spectra.

are present. Only the small shoulder at 2.5 eV is found to be due to pure surface to surface transitions. In the energy range between 2.5 eV and 4.2 eV, electron transitions from occupied surface states to empty bulk states and from bulk to surface states dominate the spectra, mainly arising from transitions along the $\bar{M}-\bar{X}'-\bar{\Gamma}$ direction in the IBZ. These theoretical findings are in agreement with very recent experiments of adsorption of cesium on InAs (Ref. 44) where it is shown that for increasing Cs coverage the experimental structures at 2.0, 3.1, and 4 eV disappear, thus confirming the surface-related nature of those peaks.

The intense peak at about 4.5 eV is described differently in TB and GW. According to TB this peak is due to surface to surface and surface to bulk transitions between the occupied A_3 surface states and the empty C_3 surface states and bulk states. According to GW, however, transitions among modified bulk states are responsible for the 4.5 eV experimental peak and just a few contributions from surface related transitions play a role. Following Cs coverage,⁴⁴ this structure has been shown to survive, although its intensity decreases somewhat. This is in agreement with the GW result that it is mainly bulk related. Furthermore, the agreement at higher energies, where both GW and experiment show a minimum, substantiates the GW description, as TB instead displays a maximum. The agreement between GW theory and experiment is good for all energies, thus showing that a good theoretical description of the electronic structure and consequently of the optical properties is possible with GW for this surface. Excitonic effects, not included in the calculation, seem not to be important. The fact that not only the

spectral structure but also the absolute values of the GW result compares well with experiment is especially noteworthy.

V. SUMMARY

We have performed an extensive theoretical and experimental study of the electronic structure and optical properties of the clean InAs(110) surface. Several theoretical techniques of increasing accuracy (and effort) have been used, ranging from tight binding to DFT and GW. An overall good agreement to experiment was found for TB, especially at intermediate energies. The *ab initio* GW approach gives remarkably good values for the electronic energies. It explains, moreover, the main features of the spectrum qualitatively and quantitatively, and relates them to the surface and bulk atomic and electronic structure.

ACKNOWLEDGMENTS

We acknowledge the partial financial support from DGAPA-UNAM Grant No. IN104201, CONACyT Grant No. 36651-E. This work has been done within the Vigoni-DAAD project and was funded in part by the EU's 6th Framework Programme through the NANOQUANTA Network of Excellence (Grant No. NMP4-CT-2004-500198). We thank INFM for CINECA CPU time and G. Onida for providing us his TB code. O.P. acknowledges financial support by INFM (Grant No. PAIS-CELEX 2003-2004).

*Author to whom correspondence should be addressed. Email address: cecilia@fisica.unam.mx

¹C. B. Duke, A. Paton, A. Kahn, and C. R. Bonapace, Phys. Rev. B **27**, 6189 (1983).

²See for example, F. Bechstedt and R. Enderlein, *Semiconductor Surfaces and Interfaces* (Akademie-Verlag, Berlin, 1988); A. Zangwill, *Physics at Surfaces* (Cambridge University Press, New York, 1992); H. Lüth, *Surfaces and Interfaces of Solids* (Springer Verlag, Berlin, 1993).

³T. J. Godin, J. P. LaFemina, and C. B. Duke, J. Vac. Sci. Technol. A **10**, 2059 (1992).

⁴X. Zhu, S. B. Zhang, S. G. Louie, and M. L. Cohen, Phys. Rev. Lett. **63**, 2112 (1989).

⁵O. Pulci, G. Onida, R. Del Sole, and A. J. Shkrebtii, Phys. Rev. B **58**, 1922 (1998).

⁶O. Pulci, B. Adolph, U. Grossner, and F. Bechstedt, Phys. Rev. B **58**, 4721 (1998).

⁷F. Bechstedt, *Principles of Surface Physics* (Springer Verlag, Berlin, 2004).

⁸C. Noguez, Phys. Rev. B **58**, 12 641 (1998); **62**, 2681 (2000).

⁹G. Cappellini, G. Satta, M. Palummo, and G. Onida, Phys. Rev. B **66**, 115412 (2002).

¹⁰C. Mailhot, C. B. Duke, and D. J. Chadi, Phys. Rev. B **31**, 2213 (1985).

¹¹R. P. Beres, R. E. Allen, and J. D. Dow, Phys. Rev. B **26**, 5207

(1982).

¹²A. I. Shkrebtii, N. Esser, M. Köpp, P. Haier, W. Richter, and R. Del Sole, Appl. Surf. Sci. **104/105**, 176 (1996).

¹³R. A. Vázquez-Nava, B. Mendoza, and C. Castillo, Phys. Rev. B **70**, 165306 (2004).

¹⁴J. L. Alves, J. Hebenstreit, and M. Sheffler, Phys. Rev. B **44**, 6188 (1991).

¹⁵B. Engels, P. Richard, K. Schroeder, S. Blügel, Ph. Ebert, and K. Urban, Phys. Rev. B **58**, 7799 (1998).

¹⁶J. Klijn, L. Sacharow, C. Meyer, S. Blügel, M. Morgenstern, and R. Wiesendanger, Phys. Rev. B **68**, 205327 (2003).

¹⁷P. Hohenberg and W. Kohn, Phys. Rev. **136**, 864 (1964).

¹⁸W. Kohn and L. J. Sham, Phys. Rev. **140**, 1133 (1965).

¹⁹R. Car and M. Parrinello, Phys. Rev. Lett. **55**, 2471 (1985).

²⁰L. Hedin, Phys. Rev. **139**, A796 (1965); L. Hedin and S. Lundqvist, Solid State Phys. **23**, 1 (1969).

²¹M. S. Hybertsen and S. G. Louie, Phys. Rev. B **34**, 5390 (1986); **38**, 4033 (1988); R. Godby, M. Schlüter, and L. J. Sham, *ibid.* **37**, 10 159 (1988).

²²X. Zhu and S. G. Louie, Phys. Rev. B **43**, 14 142 (1991).

²³H. Carstensen, R. Claessen, R. Manzke, and M. Skibowski, Phys. Rev. B **41**, 9880 (1990).

²⁴C. B. M. Andersson, J. N. Andersen, P. E. S. Persson, and U. O. Karlsson, Phys. Rev. B **47**, 2427 (1992).

²⁵C. B. M. Andersson, J. N. Andersen, P. E. S. Persson, and U. O.

- Karlsson, Surf. Sci. **398**, 395 (1998).
- ²⁶D. M. Swantson, A. B. McLean, D. N. McIlroy, D. Heskett, R. Ludeke, H. Munekata, M. Prietsch, and N. J. DiNardo, Surf. Sci. **312**, 361 (1994).
- ²⁷D. M. Swantson, A. B. McLean, D. N. McIlroy, D. Heskett, R. Ludeke, H. Munekata, M. Prietsch, and N. J. DiNardo, Can. J. Phys. **70**, 1099 (1992).
- ²⁸H. W. Richter, J. Barth, J. Ghijsen, R. L. Johnson, L. Ley, J. D. Riley, and R. Sporcken, J. Vac. Sci. Technol. B **4**, 900 (1986).
- ²⁹W. Drube, D. Straub, and F. J. Himpsel, Phys. Rev. B **35**, 5563 (1987).
- ³⁰W. Gudat and D. E. Eastman, J. Vac. Sci. Technol. **13**, 831 (1976).
- ³¹J. van Laar, A. Huizer, and T. L. van Rooy, J. Vac. Sci. Technol. **14**, 894 (1977).
- ³²C. Mailhot, C. B. Duke, and D. J. Chadi, Surf. Sci. **149**, 366 (1985).
- ³³D. E. Aspnes, J. P. Harbison, A. A. Studna, and L. T. Florez, Appl. Phys. Lett. **52**, 957 (1988).
- ³⁴M. Bockstedte, A. Kley, J. Neugebauer, and M. Scheffler, Comput. Phys. Commun. **107**, 187 (1997).
- ³⁵C. Noguez and S. E. Ulloa, Phys. Rev. B **53**, 13 138 (1996), and references therein.
- ³⁶P. Vogl, H. P. Hjalmarson, and J. D. Dow, J. Phys. Chem. Solids **44**, 365 (1983).
- ³⁷Walter A. Harrison, *Electronic Structure and the Properties of Solids* (Dover Publications, New York, 1980).
- ³⁸J.-M. Jancu, R. Scholz, F. Beltram, and F. Bassani, Phys. Rev. B **57**, 6493 (1998).
- ³⁹Landolt-Börnstein, *Numerical Data and Functional Relationships in Science and Technology*, New Series, Group III, Vol. 17a, edited by O. Madelung and K.-H. Hellwege (Springer-Verlag, Berlin, 1982).
- ⁴⁰J. R. Chelikowsky and M. L. Cohen, Solid State Commun. **29**, 267 (1979).
- ⁴¹The RAS signal is commonly given in terms of the reflectance ($\Delta R/R$) or of the complex Fresnel reflectivities ($\Delta r/r$). The latter is usually used for set-ups where both components (real and imaginary) can be measured. The two quantities are related and for small amplitudes can be given as $\Delta R/R = 2 \operatorname{Re}(\Delta r/r)$.
- ⁴²For more details, see R. Del Sole, in *Photonic Probes of Surfaces*, edited by P. Halevi (Elsevier, Amsterdam, 1995), p. 131, and references therein.
- ⁴³The value 4.3 eV has been evaluated using results from inverse photoemission experiment [1.9 eV (Ref. 29)] and from XPS measurement [-2.4 eV (Ref. 39)].
- ⁴⁴K. Fleischer, G. Bussetti, C. Goletti, W. Richter, and P. Chiaradia, J. Phys.: Condens. Matter **16**, 4353 (2004).